Turkish Journal of Chemistry

http://journals.tubitak.gov.tr/chem/

Research Article

Turk J Chem
(2019) 43: 1486 – 1502
© TÜBİTAK
doi:10.3906/kim-1905-22

Glucose oxidase immobilized biofuel cell flow channel geometry analysis by CFD simulations

Salih OBUT, Tahsin BAHAR*
Energy Institute, TÜBİTAK Marmara Research Center, Kocaeli, Turkey

Received: 09.05.2019 • **Accepted/Published Online:** 24.09.2019 • **Final Version:** 07.10.2019

Abstract: Glucose oxidase was covalently immobilized to a porous electrode, which was developed by using ferrocene functionalized polyethyleneimine, multiwall carbon nanotubes, and carbon cloth for biofuel cell applications in our recent studies. The kinetics parameters (i.e. k_M, V_{max}) and other parameters required for the modeling study were determined experimentally. Fuel cell flow channel geometry was analyzed by a computational fluid dynamics modeling approach. Substrate flow rate and mass transfer for each proposed channel type were considered in the simulations. The results showed that serpentine type flow channels are advantageous over pin type or parallel flow channels to acquire sufficient performance from the immobilized enzyme electrode at lower substrate flow rates. On the other hand, a disadvantage of using serpentine type channels was observed as higher pressure drops. However, such pressure drops were accepted as reasonable for the considered flow rates for suitable biofuel cell performance.

Key words: Glucose oxidase, enzyme immobilization, bioanode, enzymatic fuel cell, flow channels, graphite plates, computational fluid dynamics, modeling, current collector

1. Introduction

Enzyme catalyzed oxidation/reduction reactions with electron transfer through a circuit could be utilized for electrochemical energy production and biosensor applications. The concept has been applied successfully in biosensor applications so that many enzymatic biosensors have become commercially available. Research on biofuel cells is also continuing with an increasing rate in scientific areas. The working principle of biofuel cells is similar to that of conventional fuel cells; however, immobilized enzymes are utilized as catalysts in the place of precious metal (Pt, etc.) catalysts. Biofuels (generally sugars) are oxidized at the anode and electrons along with protons are released. These electrons, carried through an external circuit to the cathode, are utilized with the oxidant (typically oxygen) and protons to produce a product (water) [1–5]. Glucose oxidase, among other oxidoreductases, is very popular in biofuel cell studies since both the enzyme and the substrate (i.e. glucose) are easily accessible in nature [6–10]. Attention to enzymatic fuel cells has been inspired mostly by medical applications requiring low power [9–11]. Also, some studies showed that several mW/cm^2 power densities were reachable with multistack fuel cells for powering some portable electronic equipment [12].

A deeper understanding of enzymatic redox reactions with advanced techniques in electrochemistry allows improvement of assembling biofuel cells. Mathematical modeling generally helps in this process. Many works have been conducted for the modeling of hydrogen or methanol fuel cells, but only a small number of modeling studies have been performed on enzymatic biofuel cells [9–11]. Models supported by experimental data have been

*Correspondence: tahsin.bahar@tubitak.gov.tr

This work is licensed under a Creative Commons Attribution 4.0 International License.

not only very useful for examining the microenvironment and designing new electrodes, but also for improving other important parts of the enzymatic biofuel cells. On the other hand, these models have been highly simplified, neglecting some important features such as the dynamics, nonuniformities, or ion migration [2,9–11]. A larger electrode surface area with high enzyme loadings is generally required for enhanced electrochemical performance, but modeling studies with finite element analysis showed that it was important to optimize the electrode geometry and configuration to obtain uniform current density distribution by enhanced mass transport and improved reaction kinetics for optimized enzymatic fuel cell performance [13,14]. For example, optimized fuel cell performance was obtained when the well width was half of the height of the 3D electrode and a semielliptical electrode was favored [15]. In another biofuel cell modeling study, a mathematical model considering diffusion and reaction processes confirmed the effect of the large surface area of the electrode with a thin, grafted redox polymer layer. It was found that the rate-limiting step of electron diffusion could be defeated by an electrode with a thin redox polymer [16]. Chan et al. developed a dynamic model simulating the discharge performance of an anode with supported glucose oxidase and mediator immobilization in the enzymatic biofuel cell [17]. Saranya et al. established a mathematical model of an enzymatic biofuel cell without a membrane through direct electron transfer. The significant point of this study was the description of a new homotopy perturbation method for solving nonlinear differential equations [18]. Rubin also prepared a model for direct electron transfer biofuel cells to estimate current, voltage, and power performance [19].

In this study, a computational fluid dynamics (CFD) modeling strategy was utilized to suggest the optimized flow channel type for a biofuel cell with a bioanode involving glucose oxidase. Glucose oxidase was immobilized covalently by aldehyde groups of the electrode, which was developed by using ferrocene carboxaldehyde, polyethyleneimine, multiwall carbon nanotubes, and carbon cloth as described in our recent studies [7,8]. Ideally, the substrate (glucose) should reach the entire surface area of the electrode, from top to bottom, to react with the enzyme embedded on it. Flow channel geometry for substrate transport is very important and should be carefully designed to provide sufficient properties for glucose transport to the electrode surface. Accordingly, graphite current collector plates with alternative flow channel structures were evaluated and analyzed by CFD with embedded chemical reactions. This study is one of the few computational studies on the effects of flow channel type analysis for enzymatic biofuel cells, and the results are intended to provide important information for the design and fabrication of similar types of enzymatic biofuel cells.

2. Materials and methods

2.1. Materials

D-Glucose (G8270-Sigma), glucose oxidase (G2133 Sigma, type VII from *Aspergillus niger*), polyethylenimine (482595 Aldrich), multiwalled carbon nanotube (MWCNT) (724769 Aldrich), and glutaraldehyde (G6257 Sigma-Aldrich) were bought from Sigma-Aldrich. Carbon cloth was obtained from ElectroChem Inc. (Woburn, MA, USA). Ferrocene carboxaldehyde (98%) was supplied by Acros Organics (Belgium). Other chemicals were of analytical grade. Distilled-deionized (DI) water was utilized in all experiments.

2.2. Preparation of enzymatic anode and glucose oxidase crosslinking

The glucose oxidase immobilized electrode was produced by our recently developed procedure [7,8]. Typically, 0.4 g of ferrocene carboxaldehyde dissolved in 5 mL of methanol was added gradually into 45 mL of 10% (w/w) BPEI (dissolved in methanol) solution to react with amine groups at 25 °C. The resulting medium was

agitated for 24 h at 100 rpm to complete the reaction. A reduction reaction was further completed with sodium borohydride (as a reducing agent to react the iminium species that form between the amines and ferrocene carboxaldehyde) [7,8,20]. Cleaned and soaked (with methanol) MWCNTs were equally layered on carbon cloth (5 cm^2) physically with suitable blades. The Fc-BPEI/MetOH solution obtained above was added (i.e. 0.5 mL including 40 mg mL^{-1} BPEI-Fc) to MWCNTs layered (10 mg dry basis) on carbon cloth surface for the adsorption of Fc-BPEI by MWCNTs, and 25% glutaraldehyde solution was employed (30 min at 25 °C) to tightly crosslink and to activate adsorbed Fc-BPEI. This technique not only allowed MWCNTs to embed on the carbon cloth but also provided active free aldehyde moieties for glucose oxidase immobilization [7,8,21]. The produced electrode was cleaned thoroughly with water to remove unreacted glutaraldehyde and all other chemicals from earlier processes. Then the electrodes were put into the glucose oxidase solutions (i.e. 2 mL, 20 mg enzyme/mL, buffer solution at pH 5–7) for the immobilization process. Glucose oxidase was immobilized by the Schiff base reaction between amine groups of the enzyme and the active aldehyde groups on the electrode surface. The immobilization process was conducted for 24 h at 4 °C. The immobilized enzyme (i.e. protein) amount was determined by the Biuret method [22]. The produced enzyme anode was washed extensively with suitable buffers to remove unbound glucose oxidase. The enzyme electrode was kept at 4 °C in the buffer solution before use.

2.3. Determination of glucose oxidase activity and kinetic parameters

Glucose oxidase enzymatic activity and kinetic parameters were determined by conventional (chemical) and electrochemical methods. In the conventional method, enzymatic activity (i.e. U, micromole glucose hydrolyzed/min/mg protein) of immobilized glucose oxidase on the electrode was determined by measuring glucose concentration decrease by time in batch reactors. A definite amount of enzyme immobilized electrode (i.e. 1 cm^2, 2.5 mg of total protein content) was put into the batch reactor with suitable glucose solution (200 mM, 25 mL) at suitable pH, temperature (i.e. 35 °C, pH 5), and stirring rate (i.e. 200 rpm). In the electrochemical method, electrochemical data were taken by using batch reactors (half-cell for anode) with proper temperature and pH (i.e. 35 °C, pH 5) by using a potentiostat/galvanostat system (Gamry Instruments, Inc., Reference 600R). A three-electrode configuration was utilized with the enzyme electrodes (typically 1.0 cm^2). A platinum wire was used as the counter electrode and saturated Ag/AgCl was used as the reference electrode. Open circuit potential, chronoamperometry, linear sweep voltammetry, and short-circuit current measurements were performed to determine kinetic parameters and other properties of the immobilized enzyme electrode for the modeling study [19,20].

3. Results and discussion

3.1. Model development

Power generation with enzymatic biofuel cells is proportional to the electrode surface area that provides space for the substrate (i.e. fuel) to react with the immobilized enzyme on the electrode. Interaction of the substrate with the electrode depends on the enzyme reaction rate and its amount immobilized onto the electrodes [2]. An electrode structure with a high amount of immobilized enzyme has an advantage for obtaining high power density. Ideally the substrate should react with the whole surface area of the electrode to fully utilize the immobilized enzyme. On the other hand, flow channel geometries for substrate transport are also very important and should be carefully designed to provide sufficient glucose transport to the electrode surface. Improper

selection of flow channel geometry together with a high reaction rate and loadings of enzymes permit inefficient performance because of the deficiency of fuel (i.e. glucose) on the electrode surface. Therefore, the CFD modeling strategy was utilized to provide and suggest an optimized configuration with respect to glucose concentration in this study. The model considers enzyme reactions and diffusion of the substrate in three-dimensional substrate channel geometry. Two approaches according to the reaction mechanisms (depending on electron and proton transfer routes) for the substrate utilization of the immobilized glucose oxidase were taken into account.

In the first case, enzyme reactions proceed via electron transfer through the outer electrical circuit according to Eqs. (1)–(4) instead of the conventional enzymatic reactions given in Eq. (5) and Eq. (6) [7,8,23]. Eqs. (1)–(4) describe a mediated enzymatic reaction mechanism in which the immobilized mediator (ferrocene on PEI) transfers the electron from the active site of the enzyme (FAD: flavin adenine dinucleotide) to the electrode and circuit [23].

$$GOx(FAD) + glucose \rightarrow GOx(FADH_2) + gluconolactone \tag{1}$$

$$GOx(FADH_2) + 2Fc^{+}PEI \rightarrow GOx(FAD) + 2Fc - PEI + 2H^{+} \tag{2}$$

$$2Fc - PEI + 2Fc^{+}PEI \rightarrow 2Fc^{+} - PEI + 2Fc - PEI \tag{3}$$

$$2Fc - PEI \rightarrow 2Fc^{+} - PEI + 2e^{-} \tag{4}$$

In the second case, the enzyme reaction precedes by conventional enzymatic reactions (i.e. Eq. (5) and (6)), where enzymes do not need electron transfer through the electrical circuit. Reactions are completed by the conversion of dissolved oxygen to hydrogen peroxide and electron/proton transfer occurs between the substrate solution and the enzyme active center (FAD).

$$GOx(FAD) + glucose \rightarrow GOx(FADH_2) + gluconolactone \tag{5}$$

$$GOx(FADH_2) + O_2 \rightarrow GOx(FAD) + H_2O_2 \tag{6}$$

When there is dissolved oxygen in the substrate solution, these reaction routes both likely occur at the fuel cell application, but the desired first route should be dominant to obtain high current and power densities from the cell. A higher polarization between the electrodes and more effective electron transfer to the electrode than electron transfer to the solution will force the electrochemical route.

Three main flow channel structures (mixing type serpentine, parallel, and pin type) were studied (Figures 1a–1d). A numerical model that solves the Navier–Stokes equations with species transport equations was developed. The consumption rate of glucose was implemented by using the user-defined function capability of the commercial software package ANSYS FLUENT. The Navier–Stokes equation for the conservation of mass and momentum for steady, laminar, incompressible flow is given in Eq. (7) [24].

$$\frac{\partial \rho}{\partial t} + \nabla \bullet (\rho \vec{v}) = S_m \tag{7}$$

Here, ρ is density, $\vec{v}$ is the velocity vector, and S_m is the mass transfer source term.

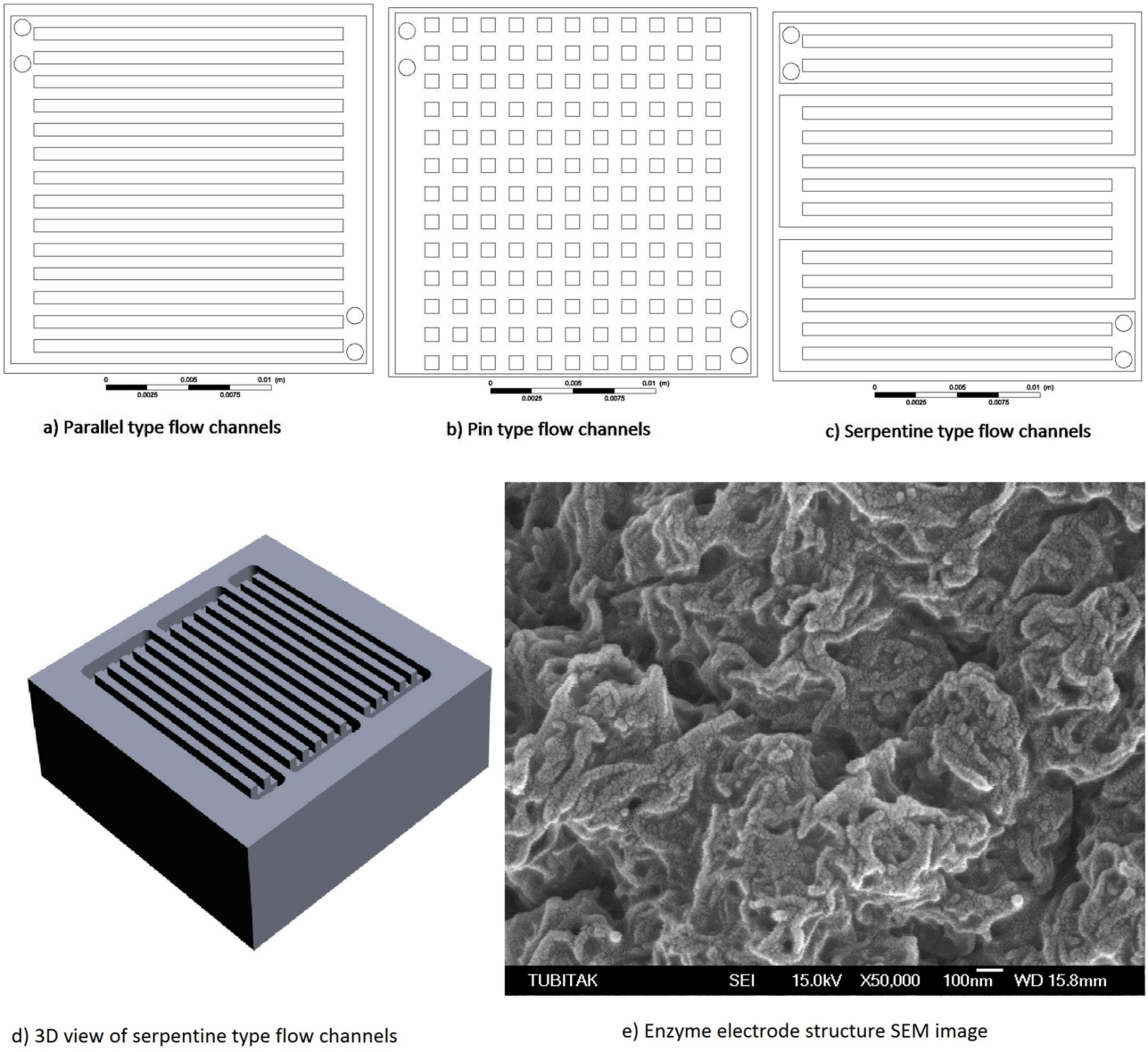


Figure 1. Geometric description (2D and 3D views) of modeled flow channels (active electrode area: 5 cm^2, channel depth: 1 mm) and SEM image (50,000 ×) of the enzyme electrode structure.

A continuity equation along with momentum conservation was used for numerical analysis. The momentum equation is given in Eq. (8).

$$\frac{\partial}{\partial t}(\rho\vec{v}) + \nabla \bullet (\rho\vec{v}\vec{v}) = -\nabla P + \nabla \bullet \left(\overline{\overline{\tau}}\right) + \rho g + \vec{F} \tag{8}$$

Here, P is pressure, $\overline{\overline{\tau}}$ is the stress tensor, g is a gravity constant, and $\vec{F}$ is force sources (momentum sources). To solve Eq. (8) in the electrode, the Darcy equation was used (Eq. (9)).

$$\nabla P = -\frac{\mu}{K}\vec{v} \tag{9}$$

Here, μ represents solution viscosity and K represents the permeability of the electrode. Glucose transport was solved by the species transport equation (Eq. (10)).

$$\frac{\partial}{\partial t}(\rho Y_{GL}) + \nabla \bullet (\rho \vec{v} Y_{GL}) = -\nabla \bullet \vec{J}_{GL} + R_{GL} \tag{10}$$

Here, Y_{GL}, $\vec{J}_{GL}$, and R_{GL} correspond to glucose mass fraction, mass transfer flux, and consumption rate ($kg/m^3/s$), respectively.

The SIMPLE algorithm based on the finite volume method was used to solve the continuity, the momentum, and the species transport equations. A second-order upwind scheme was used for discretization of convective terms and a second-order accurate scheme was used for diffusive terms. For each channel type, an unstructured mesh was generated with different sizes and a mesh independence study was performed [25].

The glucose diffusion coefficient was used as 0.2×10^{-9} m^2/s and for the electrode (Figure 1e) it was modified by porosity, as given in Eq. (11).

$$D_{GL}^{eff} = \epsilon^{1.5} D_{GL} \tag{11}$$

Geometric properties of the flow channels for CFD study are presented in Figure 1 and experimental data for enzyme kinetics (for both approaches) and other parameters are given in the Table. Once the enzyme mass balance is considered and quasi-state conditions are assumed for the reduced form of the enzyme and the enzyme–substrate complex, the rate of enzyme reaction is calculated by the Michaelis–Menten model given in Eq. (12).

$$V_{Enzyme} = \frac{V_{max}\,\mathrm{S}}{\mathrm{k}_M + \mathrm{S}} \tag{12}$$

Here, V_M is the apparent maximum reaction rate, k_M represents the apparent Michaelis constant (sensitivity or affinity of the enzyme to the substrate), and S is the substrate (glucose) concentration. Moreover, glucose consumption and current densities depending on substrate concentration via the Michaelis–Menten model can be written as given in Eqs. (13) and (14) [24].

$$R = \frac{R_{max}\,\mathrm{S}}{\mathrm{k}_M + \mathrm{S}} \tag{13}$$

$$I = \frac{I_{max}\,\mathrm{S}}{\mathrm{k}_M + \mathrm{S}} \tag{14}$$

If the substrate concentration is sufficiently high when compared to k_M ($\mathrm{S} >> \mathrm{k}_M$), the Michaelis–Menten kinetic effects could be neglected and the reaction rate approaches zeroth order. This situation is favorable but not always the case in enzymatic processes. Especially if effective substrate transfer is not achieved, substrate concentrations will approach zero [24].

A biofuel cell must also contain a suitable cathode, where the protons and electrons released at the anode are processed in order to run a closed electrical circuit. This requirement is generally fulfilled by O_2-reduction at the cathode in conventional fuel cells. O_2-reduction can easily be accomplished by cathodes bearing a conventional Pt-C catalyst. Such a conventional Pt-C cathode reaction rate is much faster than the enzymatic reaction rate and the cathode side of the biofuel cell is not a limiting part [9].

Table 1. Simulation parameters.

Enzyme electrode thickness	0.4 mm
Electrode porosity	0.4
Active electrode area	5 cm^2
Kinetic parameters For chemical case [7] For electrochemical case [8]	V_{max}: 29.48 U (micromole glucose converted/min/mg protein) k_M: 61.74 mM I_{max}: 2.77 A/cm^2 k_M: 24.61 mM
Glucose feed concentration	200 mM
Glucose diffusivity	0.2×10^{-5} cm^2/s
Temperature	35 °C
pH	5
Enzyme loading	2.4 mg/cm^2

3.2. Simulation results for enzyme kinetics controlled by electrochemical processes

In the first case (i.e. electrochemical case), the model was simulated by using the electrochemical parameters of k_M and V_M as described in the Table. Substrate feed solution glucose concentration was chosen as 200 mM since it was a realistic situation according to the enzyme kinetic parameters (Table) and laboratory experimental results. The effect of substrate solution flow rate and the relationship between the flow rate and glucose concentration were evaluated. Glucose concentration contours (Figures 2a–2d) in the anode midplane for different flow rates (1, 5, 10, 20 mL/min) were obtained by CFD simulations for the serpentine flow channels at first. It was observed from Figure 2a that when the substrate solution flow rate was 1 mL/min, the glucose concentration would be very low (less than the k_M value of the immobilized enzyme) in the lower parts of the support zones, especially between the flow channels. At this flow rate, some parts of the electrode reach sufficient glucose concentrations, but for other parts the glucose transport rate to the electrode surface is less than required to reach the immobilized enzyme's maximum reaction rate (Figure 2a) according to Michaelis–Menten kinetics (Eq. (13)).

When the flow rate was increased to 5 mL/min, the glucose concentration at the midplane of the electrode was close to the feed concentration in the majority of the electrode. After the flow rate was increased further to 10 mL/min, almost all of the electrode could remain at the equivalent glucose concentration, which was also appropriate to reach the maximum enzymatic reaction rate. Flow rates higher than 10 mL/min were thus determined as favorable since there was no substrate limitation (Figures 2c and 2d) and the reaction rate could be accepted as zeroth order according to the Michaelis–Menten kinetics (i.e. substrate concentration was sufficiently higher than k_M of the immobilized enzyme).

Similar analyses were repeated for the anode current collector plate having parallel flow channels and glucose concentration contours in the anode midplane for different flow rates were obtained (Figures 3a–3d). While the substrate solution flow rate was 1 mL/min, the glucose concentration was very low throughout the electrode (Figure 3a). When the flow rate was increased to 5 mL/min, the glucose concentration at the midplane of the electrode was still low to obtain a suitable enzymatic performance since the glucose concentration was close to the k_M of the enzyme. After the flow rate was increased to 10 mL/min, the glucose concentration reached a suitable range, but it was still not enough for favorable or optimum performance. Only after the flow

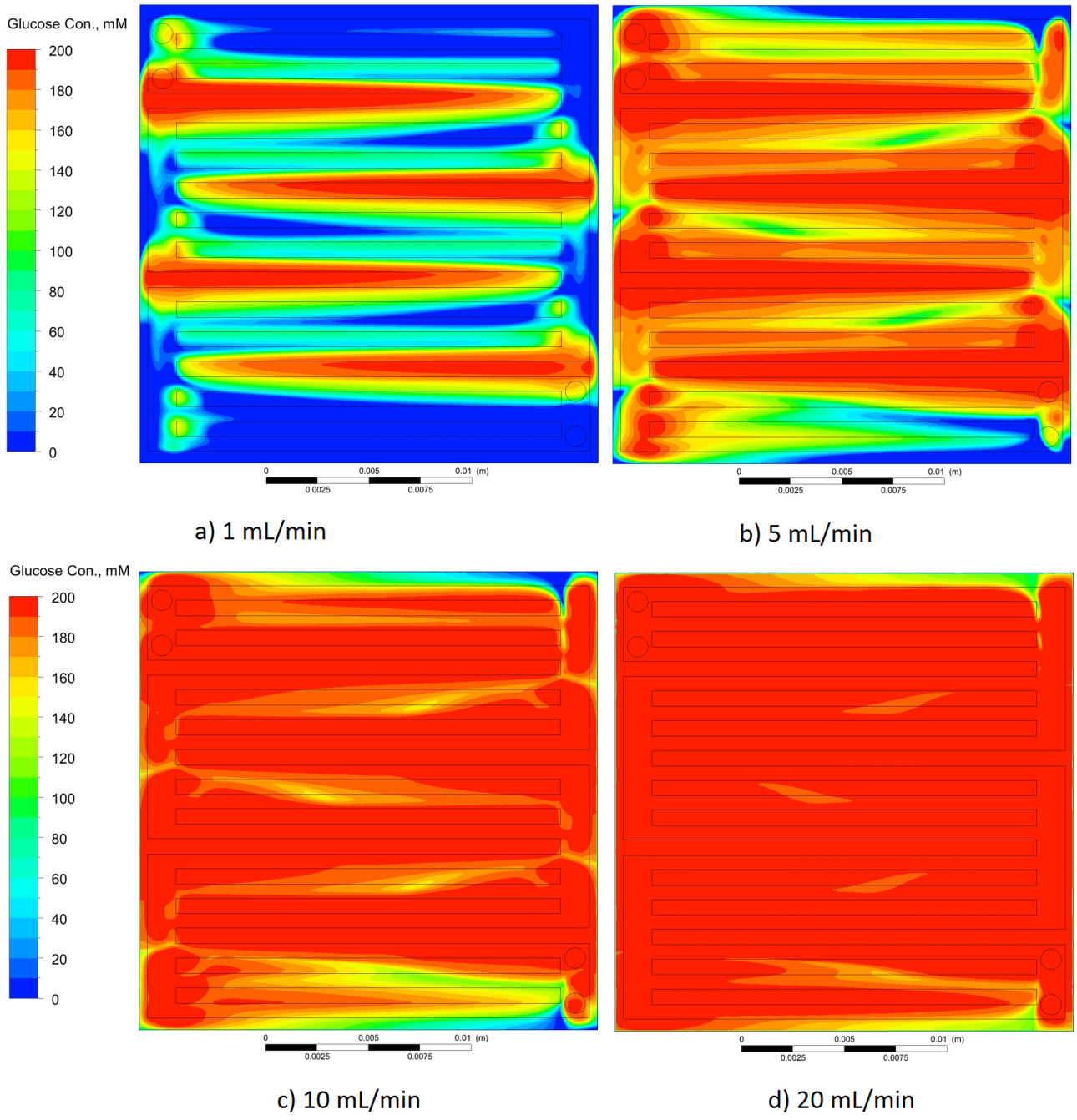


Figure 2. Simulation results for glucose concentration in the midplane of the electrode with serpentine type flow channels for electrochemical reaction mechanism case (substrate feed rate: 1–20 mL/min).

rate was increased to 20 mL/min did the glucose concentration reach a suitable range.

Finally, the pin type flow channel structure was examined similarly. Figures 4a–4d show the distribution of glucose concentration in the electrode midplane for the pin type flow channels. When the k_M of the immobilized enzyme was considered, glucose concentration deficiency for suitable enzymatic performance was observed between 1 and 10 mL/min flow rates in the regions except the input and output ports (lower left and

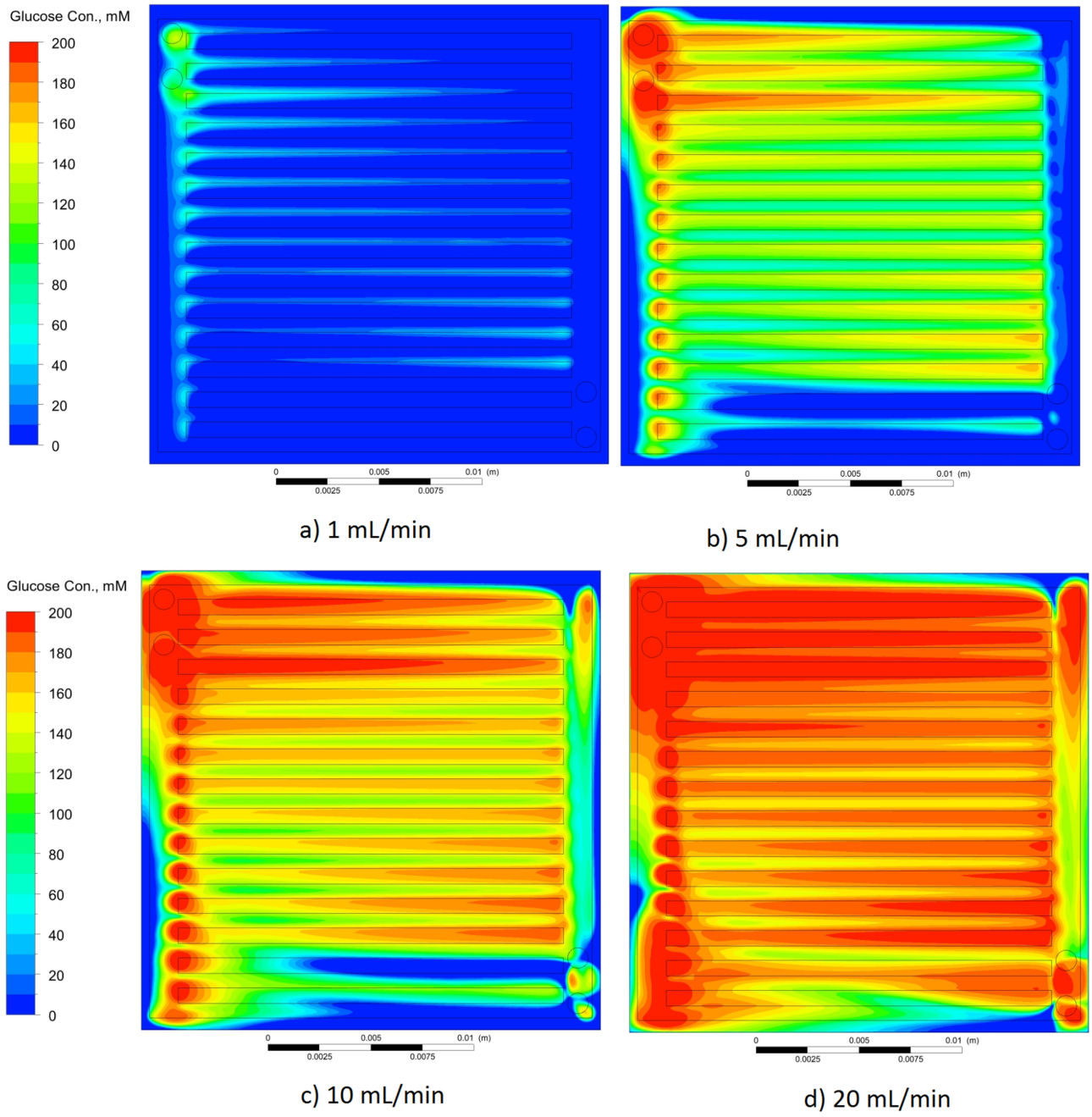


Figure 3. Simulation results for glucose concentration in the midplane of the electrode with parallel flow channels for electrochemical reaction mechanism case (substrate feed rate: 1–20 mL/min).

upper right sections according to the views in Figure 4). Only after the flow rate was increased to 20 mL/min did the glucose concentration reach an almost suitable range. As the resistance to flow in the pin type flow channels was low, the glucose solution passed through the diagonal region between the input and output ports, where the shortest distance and the least flow resistance were encountered.

Average glucose concentrations for each flow rate for each channel type were compared, as given in Figure 5. It was determined that 10 mL/min flow rate was suitable for the desired performance when the k_M of the immobilized enzyme was considered with serpentine type flow channels. For parallel and pin type channels,

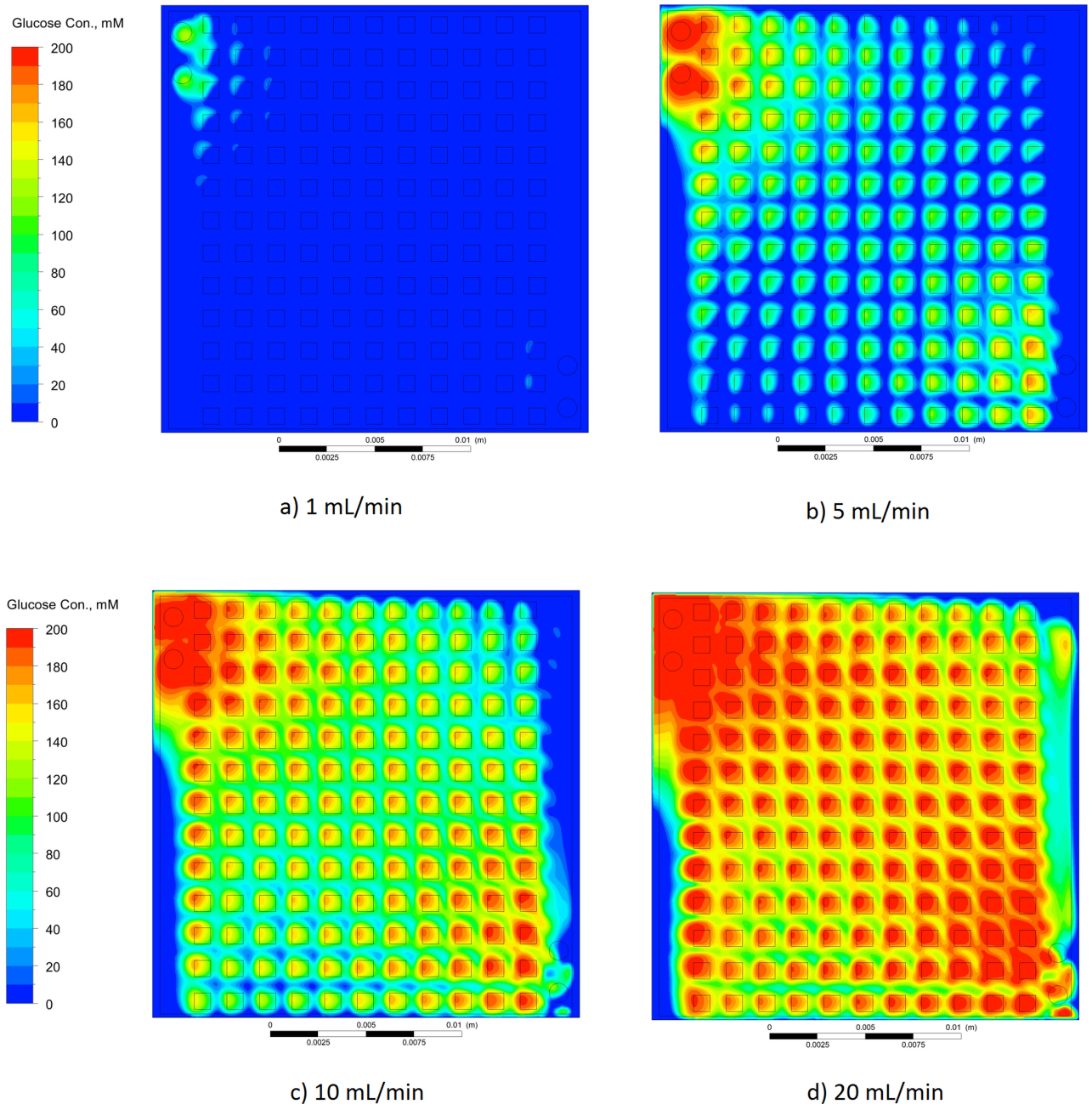


Figure 4. Simulation results for glucose concentration in the midplane of the electrode with pin type flow channels for electrochemical reaction mechanism case (substrate feed rate: 1–20 mL/min).

even 20 mL/min was relatively sufficient.

The main reason for such differences in the glucose profiles of the electrode for different flow channels was related to the glucose consumption rate that was controlled by the glucose transport to the electrode. Linear velocity of the substrate solution was higher for the serpentine type flow so the glucose transfer from the bulk solution to the electrode surface was high because of the thin mass transfer film layer. Pressure losses in the channels were also evaluated, as given in Figure 6 for each channel type and flow rate. Increase in the pressure

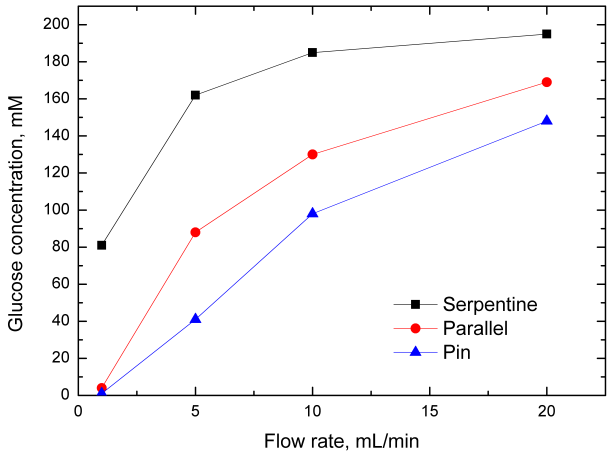


Figure 5. Simulation results for average glucose concentration in the midplane of the electrode for electrochemical reaction mechanism case.

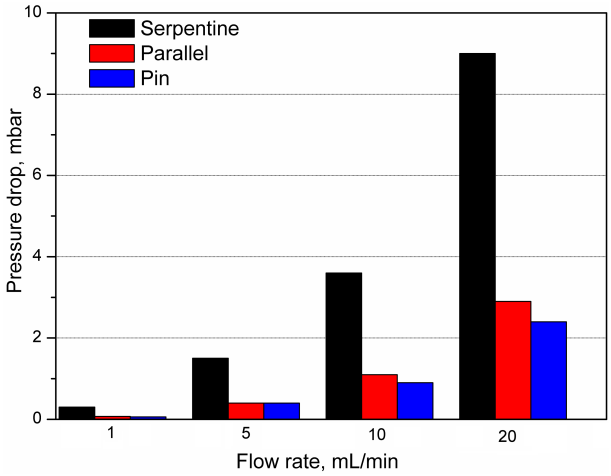


Figure 6. CFD simulation results for pressure drops at different types of flow channels for electrochemical reaction mechanism case with different flow rates.

drop with the increase of the flow rate was observed for all channel types, as expected. On the other hand, pressure drop with serpentine type flow channel was found as very sensitive to flow rate as expected.

3.3. Simulation results for enzyme kinetics controlled by conventional chemical processes

In the second simulation case, the model was simulated by using the conventional kinetic parameters instead of the electrochemical kinetic parameters of k_M and V_M described in the Table. Therefore, enzymatic reactions or glucose consumption were not controlled by electron transfer through the circuit. The system was controlled by electron and proton transfer between the enzyme and the surrounding solution, and the immobilized glucose oxidase conventional kinetics (i.e. reactions given in Eqs. (5) and (6)) were effective for the reaction rates.

Glucose concentration contours in the anode midplane for different flow rates (1, 10, 20, and 40 mL/min) were simulated for the serpentine flow channel first (Figures 7a–7d). It can be observed in Figure 7a that when the substrate solution flow rate was 1 mL/min, the glucose concentration could be very low in the lower parts of the support zones, especially between the flow channels. When the substrate solution flow rate was increased to 10 mL/min, the glucose concentration contour improved significantly in the electrode midplane, but the substrate flow rate was still insufficient since the glucose concentration at the midplane of the electrode was nonuniform and not enough in the majority of the electrode for suitable enzyme performance. Further increase of the substrate flow rate to 20 mL/min improved the glucose concentration and enabled an almost suitable enzymatic performance. Only after 40 mL/min did the glucose concentration in the midplane of the electrode reach a suitable value for the desired enzymatic performance. This flow rate could be considered to be proper only if the conventional enzymatic mechanism occurred at the electrode.

The same analysis was repeated for the parallel flow channels where glucose concentrations decreased to very low values in the electrode midplane (Figures 8a–8c). Insufficient glucose concentrations were observed even with the 40 mL/min substrate flow rate (Figure 8d). In the case of pin type flow channels, it was clearly perceived that the substrate flow rates in the 1–40 mL/min range were not adequate to provide sufficient performance from the electrode (Figure 9). The situation was worse than that of the parallel flow channels. Midplane average glucose concentrations for each flow rate for each channel type were also compared and the

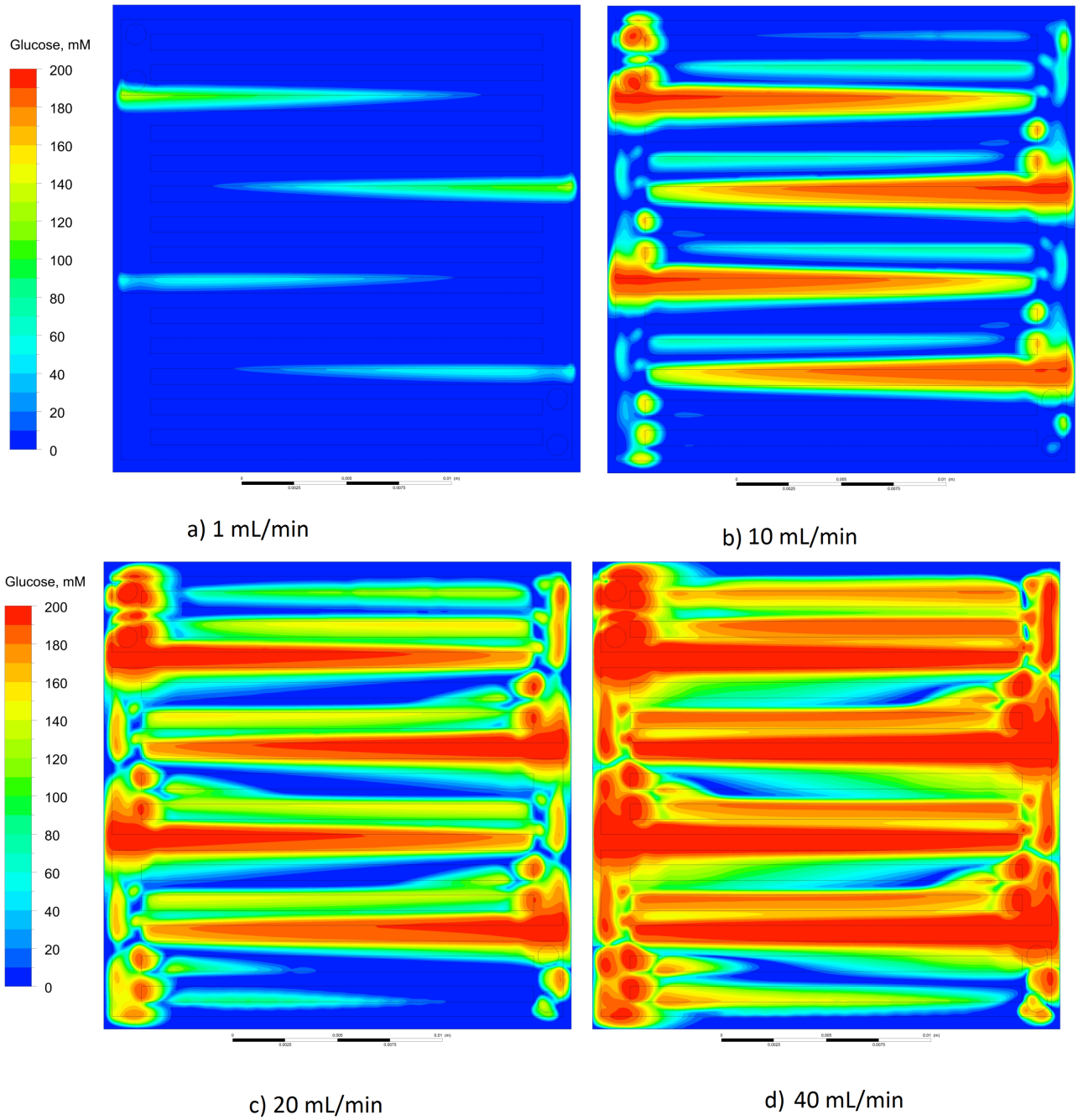


Figure 7. Simulation results for glucose concentration in the midplane of the electrode with serpentine type flow channels for chemical reaction mechanism case (substrate feed rate: 1–40 mL/min).

results are given in Figure 10. It was observed that the 40 mL/min flow rate was almost suitable for the desired performance when the k_M of the immobilized enzyme was considered with the serpentine type flow channels. On the other hand, for parallel or pin type channels the considered flow rates (1–40 mL/min) were not suitable because of insufficient glucose transport rate from the solution to the electrode. Pressure losses in the channels were also evaluated, as given in Figure 11 for each channel type and flow rate. Increase in the pressure losses

with the increase of the flow rate was also observed for all channel types, but it was more severe with the serpentine flow channel type.

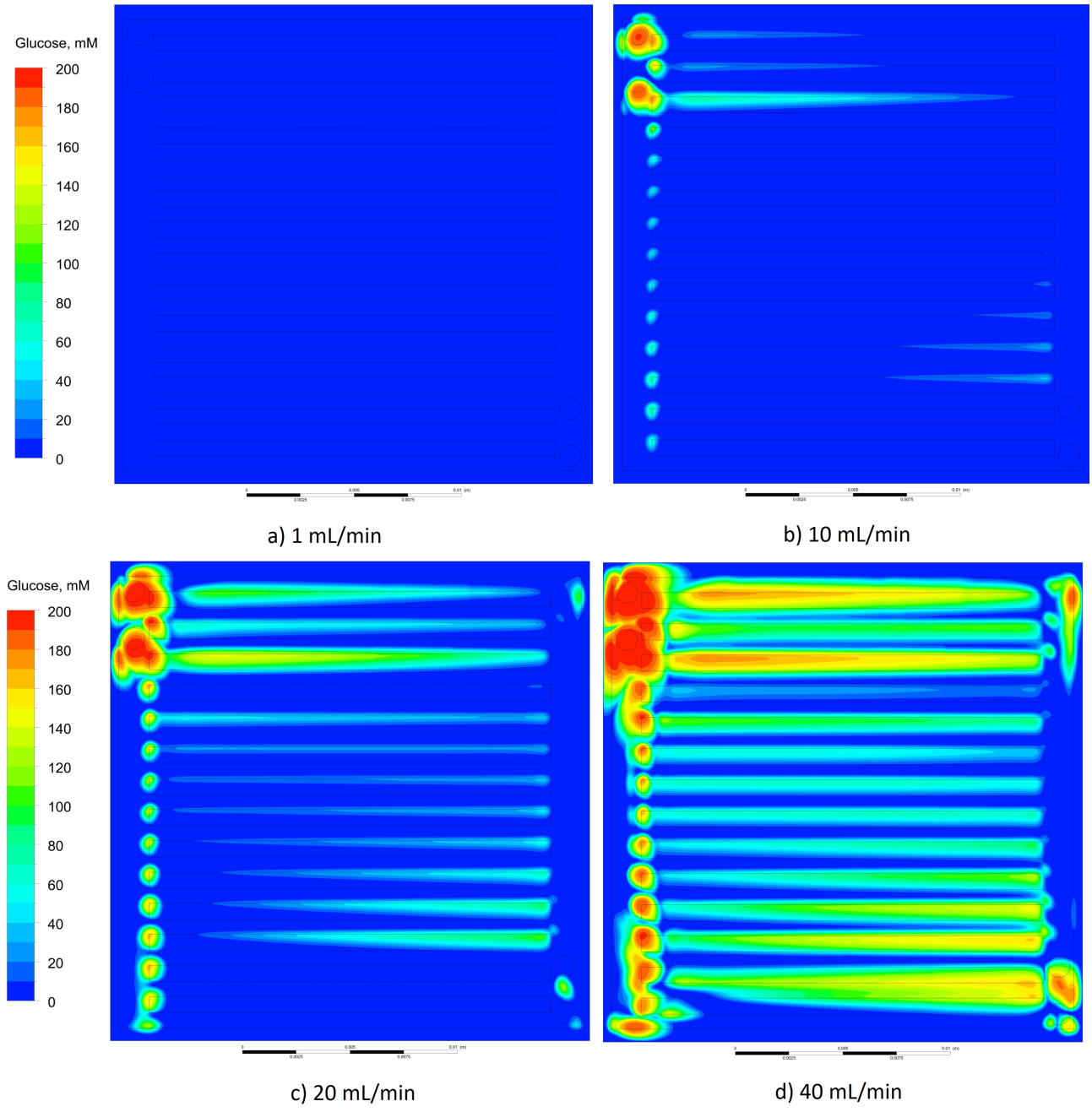


Figure 8. Simulation results for glucose concentration in the midplane of the electrode with parallel flow channels for chemical reaction mechanism case (substrate feed rate: 1–40 mL/min).

It was apparent that glucose concentrations in the electrode midplane with the conventional enzymatic reactions route (i.e. Eqs. (5) and (6)) dropped lower than those of the electrochemical reaction route (i.e. Eqs. (1)–(4)) when Figure 5 and Figure 10 were compared for identical flow rates. This result indicated that the

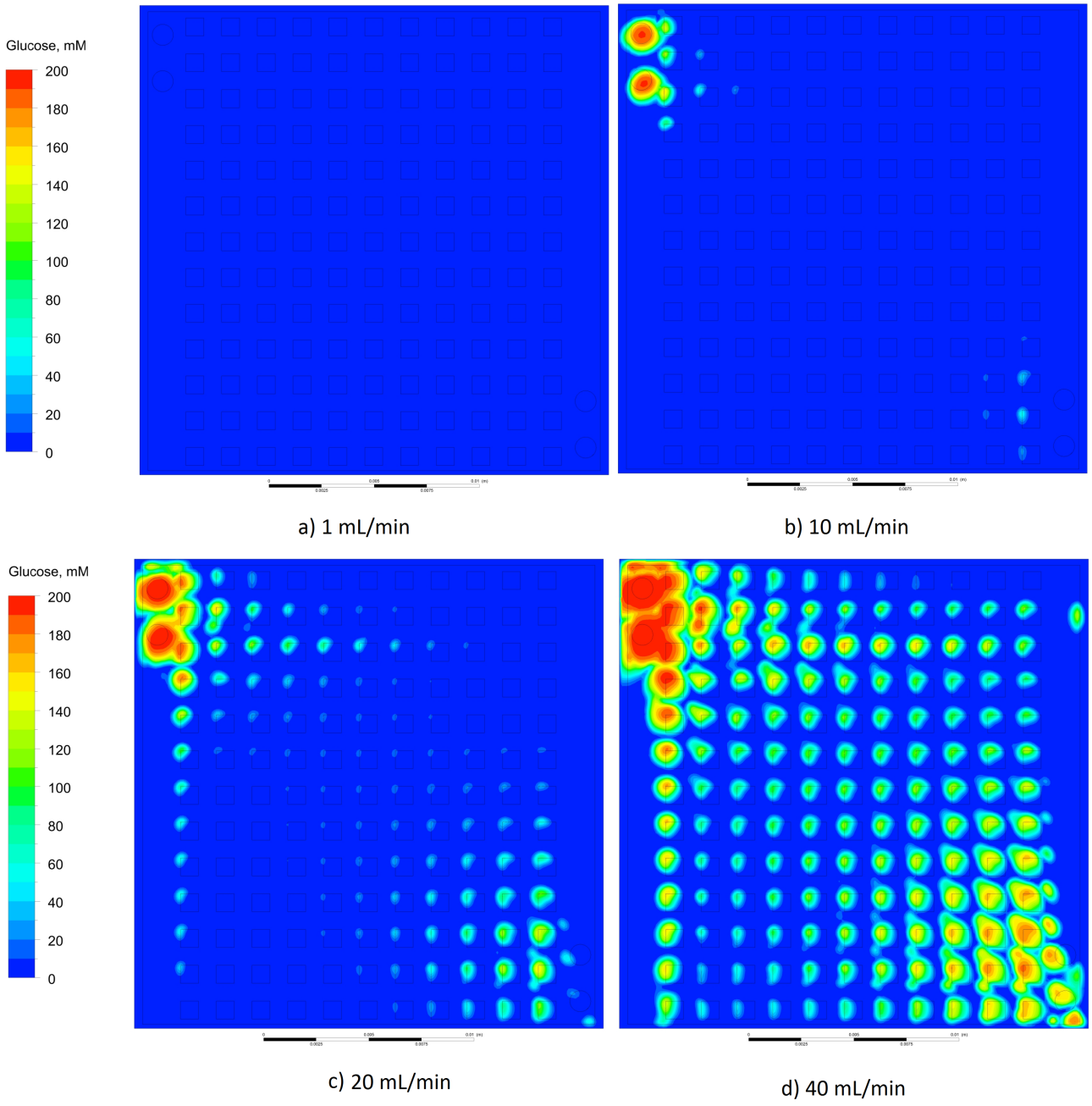


Figure 9. Simulation results for glucose concentration in the midplane of the electrode with pin type flow channels for chemical reaction mechanism case (substrate feed rate: 1–40 mL/min).

electrochemical route's glucose consumption rate was less than that of the chemical route. Dissolved oxygen is generally expected in the substrate solutions and both reaction mechanisms should be possible in the biofuel cell application. Nevertheless, the desired first route should be dominant to obtain high current densities from the cell. Higher polarization between the electrodes and more effective electron transfer to the electrode than electron transfer to the solution will enhance the domination of electrochemical route. Consequently, simulation results show that there is still some opportunity for further current density enhancement from the electrode by

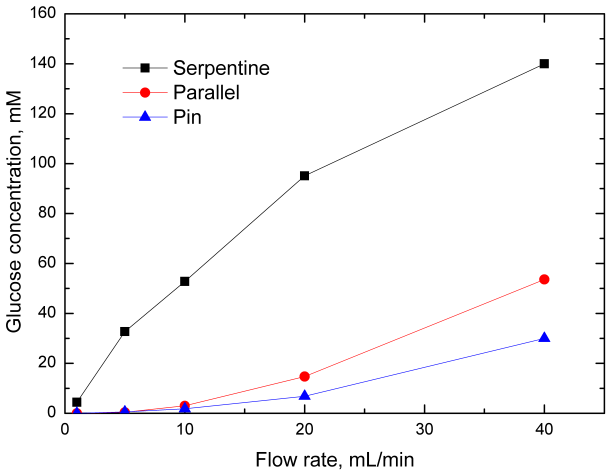


Figure 10. Simulation results for average glucose concentration in the midplane of the electrode for chemical reaction mechanism case.

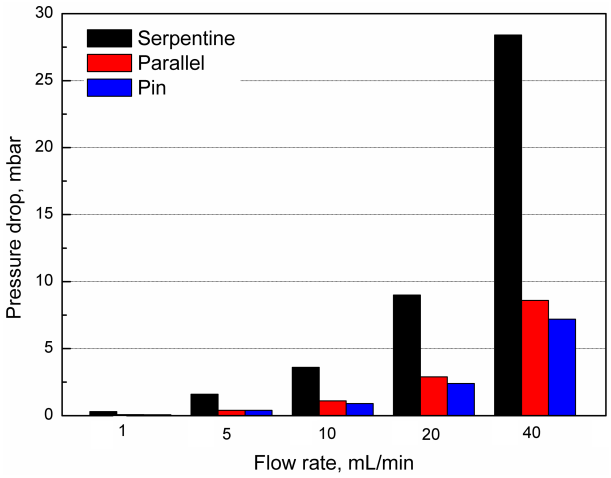


Figure 11. CFD simulation results for pressure drops at different types of flow channels for chemical reaction mechanism case with different flow rates.

improved electron transfer mechanism with immobilized enzyme electrode design.

4. Conclusion

Contours of glucose concentration in the electrode midplanes of the electrode according to the conventional enzyme mechanism were found to be quite different from those obtained on the basis of the electrochemical enzyme mechanism. These results show that there is still some room for further improvement to obtain higher current density from the cell by better electron transfer mechanism with better enzyme electrode design. It was observed that the use of serpentine type flow channels was more advantageous for this enzymatic biofuel cell system because of better glucose transport rate to the electrode surface from the substrate solution. A disadvantage of using serpentine channels and high flow rates was observed as the pressure drop (i.e. pumping power increase). Therefore, the results indicated that substrate flow rate should be optimized to obtain a sufficient performance from the electrodes in enzymatic biofuel cells.

Acknowledgment

We thankfully acknowledge the Scientific and Technological Research Council of Turkey (TÜBİTAK) for financial support provided under the TÜBİTAK 1003 Program (Project Code: 213M031).

References

1. Leech D, Kavanagh P, Schuhmann W. Enzymatic fuel cells: recent progress. Electrochimica Acta 2012; 84: 223-234. doi: 10.1016/j.electacta.2012.02.087
2. Ivanov I, Vidaković-Koch T, Sundmacher K. Recent advances in enzymatic fuel cells: experiments and modeling. Energies 2010; 3 (4): 803-846. doi: 10.3390/en3040803
3. Kavanagh P, Leech D. Mediated electron transfer in glucose oxidizing enzyme electrodes for application to biofuel cells: recent progress and perspectives. Physical Chemistry Chemical Physics 2013; 15: 4859-4869. doi: 10.1039/C3CP44617D
4. Ivnitski D, Branch B, Atanassov P, Apblett C. Glucose oxidase anode for biofuel cell based on direct electron transfer. Electrochemistry Communications 2006; 8 (2): 1204-1210. doi: 10.1016/j.elecom.2006.05.024

5. Rajendran L, Kirthiga M, Laborda E. Mathematical modeling of nonlinear reaction–diffusion processes in enzymatic biofuel cells. Current Opinion in Electrochemistry 2017; 1 (1):121-132. doi: 10.1016/j.coelec.2016.11.003
6. Kuwahara T, Ohta H, Kondo M, Shimomura M. Immobilization of glucose oxidase on carbon paper electrodes modified with conducting polymer and its application to a glucose fuel cell. Bioelectrochemistry 2008; 74 (1): 66-72. doi: 10.1016/j.bioelechem.2008.07.002
7. Bahar T. Preparation of a ferrocene mediated bioanode for biofuel cells by MWCNTs, polyethylenimine and glutaraldehyde: glucose oxidase immobilization and characterization. Asia Pacific Journal of Chemical Engineering 2016; 11 (6): 981-988. doi: 10.1002/apj.2032
8. Bahar T, Yazici MS. Immobilized glucose oxidase biofuel cell anode by MWCNTs, ferrocene and polyethylenimine: electrochemical performance. Asia Pacific Journal of Chemical Engineering 2018; 13 (1): e2149. doi: 10.1002/apj.2149
9. Gallaway JW. Mediated enzyme electrodes. In: Luckarift HR, Atanassov P, Johnson GR (editors). Enzymatic Fuel Cells: From Fundamentals to Applications. Hoboken, NJ, USA: Wiley, 2014, pp. 146-180.
10. Osman MH, Shah AA, Wills RGA, Walsh FC. Mathematical modelling of an enzymatic fuel cell with an air-breathing cathode. Electrochimica Acta 2013; 112: 386-393. doi: 10.1016/j.electacta.2013.08.044
11. Osman MH, Shah AA , Wills RGA. Detailed mathematical model of an enzymatic fuel cell. Journal of the Electrochemical Society 2013; 160 (2): F806-F814. doi: 10.1149/1.059308jes
12. Sakai H, Nakagawa, T, Tokita Y, Hatazawa T, Ikeda T et al. High-power glucose/oxygen biofuel cell operating under quiescent conditions. Energy & Environmental Science 2009; 2: 133-139. doi: 10.1039/B809841G
13. Anandan V, Yang X, Kim E, Rao Y, Zhang G. Role of reaction kinetics and mass transport in glucose sensing with nanopillar array electrodes. Journal of Biological Engineering 2007; 1: 1-10. doi: 10.1186/1754-1611-1-5
14. Godino N, Borrise X, Munoz FX, Campo FJ, Compton R. Mass transport to nanoelectrode arrays and limitations of diffusion domain approach: theory and experiment. Journal of Physical Chemistry C 2009; 113 (25): 11119-11125. doi: 10.1021/jp9031354
15. Song Y, Penmatsa V, Wang C. Modeling and simulation of enzymatic biofuel cells with three-dimensional microelectrodes. Energies 2014; 7 (7): 4694-4709. doi: 10.3390/en7074694
16. Tamaki T, Ito T, Yamaguchi T. Modelling of reaction and diffusion processes in a high-surface-area biofuel cell electrode made of redox polymer-grafted carbon. Fuel Cells 2009; 9 (1): 37-43. doi: 10.1002/fuce.200800028
17. Chan DS, Dai DJ, Wu HS. Dynamic modeling of anode function in enzyme-based biofuel cells using high mediator concentration. Energies 2012; 5 (1): 2524-2544. doi: 10.3390/en5072524
18. Saranya J, Rajendran L, Wang L, Fernandez C. A new mathematical modelling using homotopy perturbation method to solve nonlinear equations in enzymatic glucose fuel cells. Chemical Physics Letters 2016; 662: 317-326. doi: 10.1016/j.cplett.2016.09.056
19. Rubin VZ. Current-voltage modeling of the enzymatic glucose fuel cells. Advances in Chemical Engineering and Science 2015; 5 (2): 164-172. doi: 10.4236/aces.2015.52018
20. Chuang CL, Wang YJ, Lan HL. Amperometric glucose sensors based on ferrocene-containing B-polyethylenimine and immobilized glucose oxidase. Analytica Chimica Acta 1997; 353 (1): 37-44. doi: 10.1016/S0003-2670(97)00372-3
21. Bahar T. Clinoptilolite particles as a carrier for biocatalysts immobilization: invertase immobilization and characterization. Asia Pacific Journal of Chemical Engineering 2014; 9 (1): 31-38. doi: 10.1002/apj.1743
22. Ohnishi ST, Barr JK. A simplified method of quantitating protein using the biuret and phenol reagents. Analytical Biochemistry 1978; 86 (1): 193-200. doi: 10.1016/0003-2697(78)90334-2

23. Merchant SA, Meredith MT, Tran TO, Brunski DB, Johnson MB et al. Effect of mediator spacing on electrochemical and enzymatic response of ferrocene redox polymers. Journal of Physical Chemistry C 2010; 114 (26): 11627-11634. doi: 10.1021/jp911188r

24. Kjeang E, Sinton D, Harrington DA. Strategic enzyme patterning for microfluidic biofuel cells. Journal of Power Sources 2006; 158 (1): 1-12. doi: 10.1016/j.jpowsour.2005.07.092

25. Patankar, S. Numerical Heat Transfer and Fluid Flow. Boca Raton, FL, USA: CRC Press, 1980.